International Journal of Power Electronics and Drive System (IJPEDS)
Vol.2, No.2, June 2012, pp. 127~137
ISSN: 2088-8694

Adaptive Recurrent Network Network Uncertainty Observer Based Integral Backstepping Control for a PMSM Drive System

Chih-Hong Lin*, Ren-Cheng Wu*
* Departement of Electrical Engineering, National United University, Taiwan, ROC

Article Info

Article history:

Received Jan 22th, 2012
Revised Mar 12th, 2012
Accepted Mar 29th, 2012

Keyword:

integral backstepping control
permanent magnet synchronous motor
recurrent neural network

ABSTRACT

The permanent magnet synchronous motor (PMSM) is suitable for high-performance servo applications and has been used widely for the industrial robots, computer-numerically-controlled (CNC) machine tools and elevators. The control performance of the actual PMSM drive system depends on many parameters, such as parameter variations, external load disturbance, and friction force. Their relationships are complex and the actual PMSM drive system has the properties of nonlinear uncertainty and time-varying characteristics. It is difficult to establish an accurate model for the nonlinear uncertainty and time-varying characteristics of the actual PMSM drive system Therefore, an adaptive recurrent neural network uncertainty observer (ARNNUO) based integral backstepping control system is developed to overcome this problem in this paper. The proposed control strategy is based on integral backstepping control combined with RNN uncertainty observer to estimate the required lumped uncertainty. An adaptive rule of the RNN uncertainty observer is employed to on-line adjust the weights of sigmoidal functions by using the gradient descent method and the backpropagation algorithm in according to Lyapunov function. This ARNNUO has the on-line learning ability to respond to the system's nonlinear and time-varying behaviors. Experimental results are executed to show the control performance of the proposed control scheme.

Corresponding Author:

Chih-Hong Lin,
Departement of Electrical Engineering,
National United University,
No. 1 Lienda, Kungjing Village, Miao Li County 360, Taiwan, ROC.
Email: jhlin@nuu.edu.tw

1. INTRODUCTION

The AC servo drives, including PMSMs (both trapezoidal and sinusoidal types), switched reluctance motors and induction motors, have been widely used in robotics, computer-numerically-controlled (CNC) machine tools, elevators and many other applications in the area of mechatronics [1, 2] for decades. To achieve fast four-quadrant operation and smooth starting and acceleration, the field-oriented control [1-3], or vector control, is used in the design of AC servo drives. Compared with induction servo motors, a PM synchronous motor has such advantages as higher efficiency owing to the absence of rotor losses and lower no-load current below the rated speed; moreover, its decouple control performance is much less sensitive to the parameter variations of the motor [1-3].

The backstepping design provides a systematic framework for the design of tracking and regulation strategies, suitable for a large class of state feedback linearizable nonlinear systems. The approach can be extended to handle systems with unknown parameters via adaptive backstepping [4-9]. The idea of backstepping design is to select recursively some appropriate functions of state variables as pseudo-control inputs for lower dimension subsystems of the overall system. Each backstepping stage results in a new pseudo-control design, expressed in terms of the pseudo control designs from preceding design stages. When

the procedure terminates, a feedback design for the true control input results, which achieves the original design objective by virtue of a final Lyapunov function formed by summing up the Lyapunov functions associated with each individual design stage [4-5]. In addition, owing to the robust control performance of adaptive backstepping control and sliding mode control, numerous combined adaptive backstepping and sliding-mode control schemes have appeared for both linear and nonlinear systems [6-9].

The NNs can be mainly classified as feedforward neural networks (FNNs) and recurrent neural networks (RNNs) according to the structures [10-15]. It is well known that an FNN is capable of approximating any continuous functions closely. However, the FNN is a static mapping; it is unable to represent a dynamic mapping without the aid of tapped delays. The RNNs [10-15] are a general case of artificial neural networks where the connections are not feed-forward ones only. In RNNs, connections between units form directed cycles, providing an implicit internal memory. Those RNNs are adapted to problems dealing with signals evolving through time. Their internal memory gives them the ability to naturally take time into account. Valuable approximation results have been obtained for dynamical systems. The RNNs which comprise both feedforward and feedback connections, have superior capabilities than FNNs, such as dynamic behavior and the ability to store information. Since recurrent neuron has an internal feedback loop, it captures the dynamic response of a system without external feedback through delays. Thus, RNNs are dynamic mapping and demonstrate good control performance in the presence of unmodelled dynamics, parameter variations and external disturbances [10-15]. For the purpose of real-time control, a RNN with simple network structure is proposed in this study. Due to uncertainties exist in the applications of the PMSM drive system which seriously influence the control performance, thus, the ARNNUO based integral backstepping control system is proposed to control PMSM to overcome this problem in this paper.

2. CONFIGURATION OF PMSM DRIVE SYSTEM

The machine model of a PMSM can be described in the rotor rotating reference frame as follows [1-3]:

$$v_q = Ri_q + L_q \dot{i}_q + \omega_r L_d i_d \quad (1)$$

$$v_d = Ri_d + L_d \dot{i}_d - \omega_r L_q i_q \quad (2)$$

where v_d and v_q are d and q axis stator voltage, $\dot{i}_d$ and $\dot{i}_q$ are d and q axis stator current L_d and L_q are d and q axis stator inductance, R is the stator resistance, ω_r is rotor speed.

The electric torque can be expressed as

$$T_e = 3P[L_{md} I_{fd} i_q + (L_d - L_q) i_d i_q]/4 \quad (3)$$

and the equation of the motor dynamics is

$$T_e = T_L + B\omega_r + J\dot{\omega}_r \quad (4)$$

In (3) and (4), T_e is the electric torque, T_L stands for the load torque (external load disturbance), B represents the viscous frictional coefficient and J is the moment of inertia, P *is* number of poles.

The configuration of a DSP field-oriented PMSM drive is shown in Fig. 1. The system is constituted by the following parts: a PMSM (loaded with a magnet-force brake), a interlocked and delay time circuits, a field-oriented mechanism including the coordinate translation, $\sin\theta_s / \cos\theta_s$ and lookup table generation, a hysteresis-band comparison current-controlled PWM which were all implemented using TMS320C32 DSP control board, a voltage source inverter (VSI), a speed control loop and a position control loop were implemented by DSP control board. The field-oriented mechanism drive system was implemented by TMS320C32 DSP control system. A host PC downloads the program running on the DSP. A mechanism with adjustable inertia is also coupled to the rotor of the PMSM. With the implementation of field-oriented control [1-3], the PMSM drive can be simplified to a control system with block diagram shown in Fig. 2, in which

$$T_e = K_t i_q^* \quad (5)$$

$$K_t = 3PL_{md} I_{fd} / 4 \quad (6)$$

where K_t is the torque constant; i_q^* is the torque current command; T_L is the external load disturbance; ω^* and ω_r are the command speed and rotor speed, respectively.

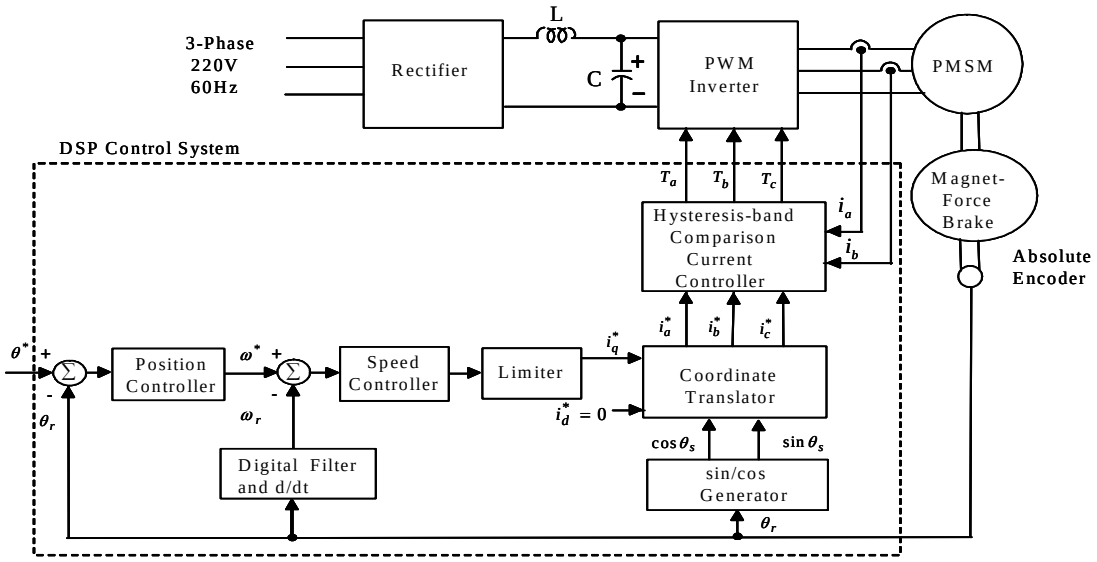

Figure 1. Configuration of DSP field-oriented control PMSM drive system

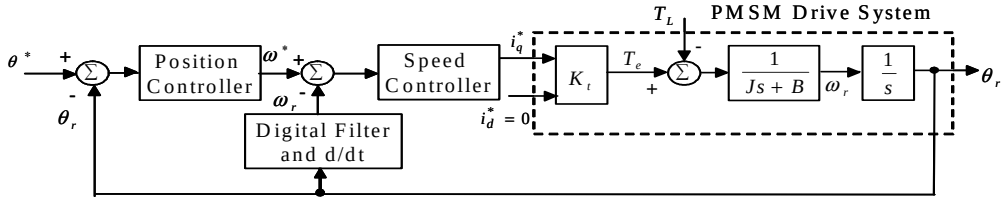

Figure 2. Simplified control system block diagram

3. RESULTS AND ANALYSIS

3.1. Integral Backstepping Control System Using Adaptive RNNUO

Consider a drive system with parameter variations, external load disturbance, and friction force for the actual PMSM servo drive system, then (4) can be rewritten as

$$\dot{\theta}_r = \omega_r = X_p \tag{7}$$

$$\dot{X}_p = (A_a + \Delta A)X_p + (B_a + \Delta B_a)U_B + C_a T_L \tag{8}$$

$$Y = \theta_r \tag{9}$$

where θ_r is the rotor position of the PMSM; X_p is the rotor velocity of the PMSM; $A_a = -B/J$; $B_a = K_t/J > 0$; $C_a = -1/J$; ΔA and ΔB denote the uncertainties introduced by system parameters J and B ; U_B is the control input to the rotor drive system. Reformulate (8), then

$$\dot{X}_p = A_a X_p + B_a U_B + H \tag{10}$$

where H is named the lumped uncertainty and defined by

$$H \equiv \Delta A X_p + \Delta B U_B + C T_L \tag{11}$$

The lumped uncertainty H will be observed by an adaptive uncertainty observer and assumed to be a constant during the observation. The above assumption is valid in practical digital processing of the observer since the sampling period of the observer is short enough compared with the variation of H.

The control objective is to design an Integral backstepping control system for the output Y of the system shown in (9) totrack the reference trajectory $Y_d(t)$, which is θ^*, asymptotically. The proposed the Integral backstepping control system is designed to achieve the position-tracking objective and described step by step as follows.

Step 1:

For the position-tracking objective, define the tracking error as

$$z_1 = \theta^* - \theta_r = Y_d - Y \tag{12}$$

and its derivative is

$$\dot{z}_1 = \dot{Y}_d - \dot{Y} = \dot{Y}_d - X_p \tag{13}$$

Define the following stabilizing function:

$$\alpha_1 = c_1 z_1 + \dot{Y}_d + c_2 \chi \tag{14}$$

where c_1 and c_2 are positive constants. $\chi = \int z_1(\tau) d\tau$ is the integral action and by using this equation we can ensure that tracking error converge to zero. The first Lyapunov function is chosen as

$$V_1 = z_1^2 / 2 \tag{15}$$

Define $z_2 = X_p - \alpha_1$, then V_1 the derivative of is

$$\dot{V}_1 = z_1(\dot{Y}_d - X_p) = z_1(\dot{Y}_d - z_2 - \alpha_1) = -z_1 z_2 - c_1 z_1^2 - c_2 z_1 \chi \tag{16}$$

Step 2:

The derivative of z_2 is now expressed as

$$\begin{aligned} \dot{z}_2 &= \dot{X}_p - \dot{\alpha}_1 = A_a X_p + B_a U_B + H - c_1 \dot{z}_1 - \ddot{Y}_d - c_2 \chi \\ &= A_a (z_2 + \alpha_1) + B_a U_B + H - c_1 \dot{z}_1 - \ddot{Y}_d - c_2 \chi \end{aligned} \tag{17}$$

To design the Integral backstepping control system, the lumped uncertainty H is assumed to be bounded, i.e., $|H| \le \overline{H}$, and define the following Lyapunov function:

$$V_2 = V_1 + z_2^2 / 2 + c_2 \chi^2 / 2 \tag{18}$$

Using (16) and (17), the derivative of V_2 can be derived as follows:

$$\begin{aligned} &\dot{V}_2(z_1, z_2) = \dot{V}_1 + z_2 \dot{z}_2 + c_2 \chi \dot{\chi} = -z_1 z_2 - c_1 z_1^2 - c_2 z_1 \chi + c_2 \chi \dot{\chi} \\ &+ z_2 [A_a (z_2 + \alpha_1) + B_a U_B + H - c_1 \dot{z}_1 - \ddot{Y}_d - c_2 \chi] \\ &= -c_1 z_1^2 + z_2 [- z_1 + A_a (z_2 + \alpha_1) + B_a U_B + H] - z_2 [c_1 \dot{z}_1 + \ddot{Y}_d + c_2 \chi] \end{aligned} \tag{19}$$

According to (19), an integral backstepping control law U_B is designed as follows:

$$U_B = B_a^{-1} [z_1 - c_2 z_2 - A_a (z_2 + \alpha_1) - \overline{H} sgn(z_2)] + B_a^{-1} (c_1 \dot{z}_1 + \ddot{Y}_d + c_2 \chi) \tag{20}$$

where c_1 and c_2 are positive constants. Substituting (20) into (19), the following equation can be obtained:

$$\dot{V}_2(z_1, z_2) = -c_1 z_1^2 - c_2 z_2^2 + z_2 H - |z_2| \overline{H} \le -c_1 z_1^2 - c_2 z_2^2 \tag{21}$$

Define the following term:

$$\Theta(t) = c_1 z_1^2 + c_2 z_2^2 \le -\dot{V}_2(z_1, z_2) \tag{22}$$

Then

$$\int_0^t \Theta(\tau) \, d\tau \le V_2(z_1(0), z_2(0)) - V_2(z_1(t), z_2(t)) \tag{23}$$

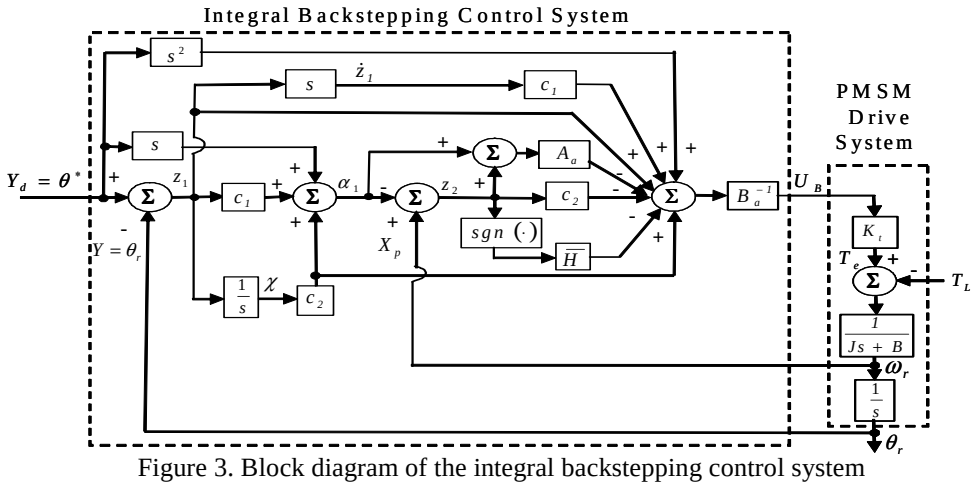

Figure 3. Block diagram of the integral backstepping control system

Since $V_2(z_1(0), z_2(0))$ is bounded, and $V_2(z_1(t), z_2(t))$ is nonincreasing and bounded, then $\lim_{t\to\infty}\int_0^t \Theta(\tau)\, d\tau < \infty$. Moreover, $\dot{\Theta}(t)$ is bounded, then and $\Theta(t)$ is uniformly continuous [16]. By using Barbalat's lemma [16], it can be shown that $\lim_{t\to\infty}\Theta(t) = 0$. That is z_1 and z_2 will converge to zero as $t \to \infty$. Moreover, $\lim_{t\to\infty} Y(t) = Y_d$ and $\lim_{t\to\infty} X_p = \dot{Y}_d$. Therefore, the integral backstepping control system, which is shown in Fig. 3, can be guaranteed.

Step 3:

Since the lumped uncertainty H is unknown in practical application, the upper bound $\overline{H}$ is difficult to determine, therefore, a RNN uncertainty observer is proposed to adapt the value of the lumped uncertainty $\hat{H}$. A three-layer RNN as shown in Fig. 4, which comprises an input (the *i* layer), a hidden (the *j* layer) and an output layer (the *k* layer), is adopted to implement the proposed control system. The signal propagation and the activation function in each layer is introduced as follows:

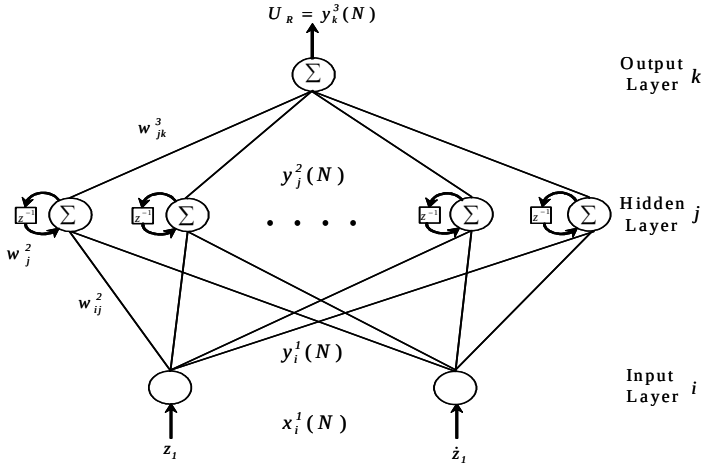

Figure 4. Network structure of RNN

Layer 1: Input Layer

$$net_i^1(N) = x_i^1(N), \quad y_i^1(N) = f_i^1\left(net_i^1(N)\right) = 1/(1+e^{-net_i^1(N)}), \quad i = 1,2 \tag{24}$$

where x_i^1 represents the *i*th input to the node of input layer; *N* denotes the number of iterations; f_i^1 is the activation function, which is a sigmoidal function. The inputs of the RNN are the tracking error z_1 and $\dot{z}_1$, which is the difference between the output of the reference model θ^* and the rotor position θ_r, and its derivative.

Layer 2: Hidden Layer

$$net_j^2(N) = w_j^2 y_j^2(N-1) + \sum_i w_{ij}^2 x_i^2(N),$$
$$y_j^2(N) = f_j^2\left(net_j^2(N)\right) = 1/(1+e^{-net_j^2(N)}), \quad j = 1,2,...,l \tag{25}$$

where w_j^2 are the recurrent weight for the units in the hidden layer; w_{ij}^2 are the connective weights between the input layer and the hidden layer; *l* is the number of neurons in the hidden layer; f_j^2 is the activation function, which is also a sigmoidal function; $y_i^1(N) = x_i^2(N)$ represents the *j*th input to the node of hidden layer.

Layer 3: Output Layer

$$net_k^3(N) = \sum_j w_{jk}^3 x_j^3(N), \quad y_k^3(N) = f_k^3\left(net_k^3(N)\right) = net_k^3, \quad k = 1 \tag{26}$$

where w_{jk}^3 are the connective weights between the hidden layer and the output layer; f_k^3 is the activation function, which is set to be unit; $y_j^2(N) = x_j^3(N)$ represents the *k*th input to the node of output layer. The output of the RNN $U_R = y_k^3(N)$ is rewritten as follows:

$$U_R = \hat{H}(\mathbf{O}) = \mathbf{O}^T \mathbf{\Gamma} \tag{27}$$

where $\mathbf{O}=\left[w_{11}^3\ w_{21}^3 \cdots\cdots w_{l1}^3\right]^T$ is the collections of the adjustable parameters of RNN. $\mathbf{\Gamma}=\left[x_1^3\ x_2^3 \cdots\cdots x_l^3\right]^T$, in which x_j^3 is determined by the selected sigmoidal function and $0 \le x_j^3 \le 1$.

To develop the adaptation laws of the RNN uncertainty observer, the minimum reconstructed error E is defined as follows:

$$E = H - H(\mathbf{O}^*) \tag{28}$$

where $\mathbf{O}^*$ is an optimal weight vector that achieves the minimum reconstructed error, and the absolute value of E is assumed to be less than a small positive constant, $\overline{E}$ (i.e., $|E| \le \overline{E}$). Then, a Lyapunov candidate is chosen as

$$V_3 = V_2 + (\hat{E}-E)^2/2\rho + (\mathbf{O}-\mathbf{O}^*)^T(\mathbf{O}-\mathbf{O}^*)/2\eta \tag{29}$$

where ρ and η are positive constants; $\hat{E}$ is the estimated value of the minimum reconstructed error E. The estimation of the reconstructed error E is to compensate the observed error induced by the RNN uncertainty observer and to further guarantee the stable characteristic of the whole control system. Take the derivative of the Lyapunov function from (29)

$$\begin{aligned}\dot{V}_3 &= \dot{V}_2 + (\hat{E}-E)\dot{\hat{E}}/\rho + (\boldsymbol{O}-\boldsymbol{O}^*)^T\dot{\boldsymbol{O}}/\eta \\ &= -c_1 z_1^{\,2} + z_2\left[-z_1 + A_a(z_2+\alpha_1) + B_a U_B + H\right] \\ &\quad - z_2[c_1\dot{z}_1 + \ddot{Y}_d + c_2\chi] + (\hat{E}-E)\dot{\hat{E}}/\rho + (\mathbf{O}-\mathbf{O}^*)^T\dot{\mathbf{O}}/\eta\end{aligned} \tag{30}$$

According to (30), an integral backstepping control with adaptive law $U_B = \hat{U}_B$ is proposed as follows:

$$\hat{U}_B = B_a^{-1}[z_1 - c_2 z_2 - A_a(z_2+\alpha_1) - \hat{E} - \hat{H}] + B_a^{-1}(c_1\dot{z}_1 + \ddot{Y}_d + c_2\chi) \tag{31}$$

Substituting (31) into (30), the following equation can be obtained

$$\begin{aligned}\dot{V}_3 &= -c_1 z_1^{\,2} - c_2\, z_2^{\,2} + z_2 H - z_2\hat{H} - z_2\hat{E} \\ &\quad + (\hat{E}-E)\dot{\hat{E}}/\rho + (\mathbf{O}-\mathbf{O}^*)^T\dot{\mathbf{O}}/\eta \\ &= -c_1 z_1^{\,2} - c_2 z_2^{\,2} - z_2(\hat{E}-E) - z_2(\mathbf{O}-\mathbf{O}^*)^T\mathbf{\Gamma} + (\hat{E}-E)\dot{\hat{E}}/\rho + (\mathbf{O}-\mathbf{O}^*)^T\dot{\mathbf{O}}/\eta\end{aligned} \tag{32}$$

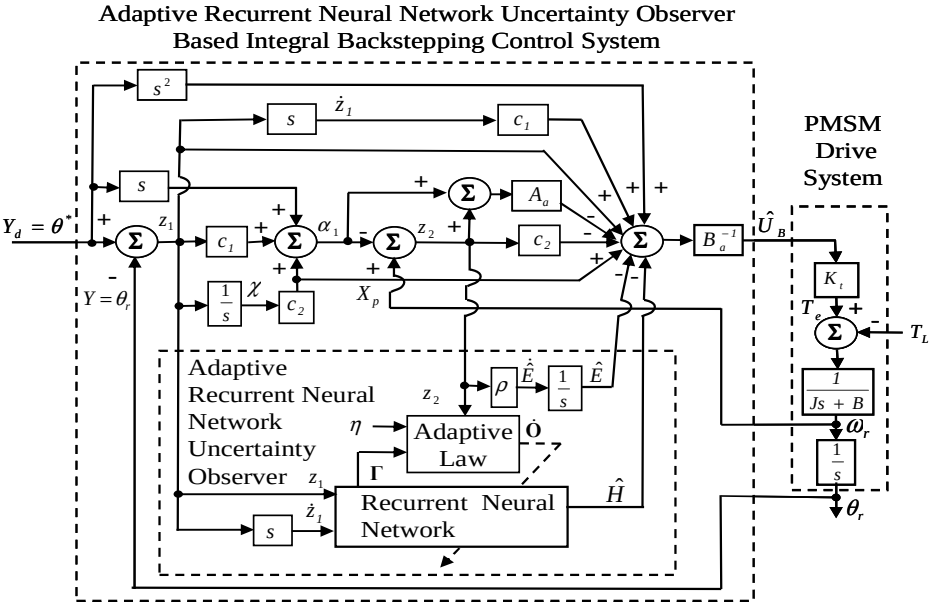

Figure 5. Block diagram of the the ARNNUO based integral backstepping control system

The adaptation laws for $\dot{\mathbf{O}}$ and $\dot{\hat{E}}$ are designed as follows:

$$\dot{\mathbf{O}} = \eta z_2 \mathbf{\Gamma} \tag{33}$$

$$\dot{\hat{E}} = \rho z_2 \tag{34}$$

Thus, (32) can be rewritten as follows:

$$\dot{V}_3 = -c_1 z_1^{\,2} - c_2\, z_2^{\,2} = \Theta(t) \le 0 \tag{35}$$

By using Barbalat's lemma [16], it can be shown that $\Theta(t) \to 0$ as $t \to \infty$. That is z_1 and z_2 will converge to zero as $t \to \infty$. As a result, the stability of the proposed the the ARNNUO based integral backstepping control system, which is shown in Fig. 5, can be guaranteed. On the other hand, the guaranteed convergence of tracking error to be zero does not imply convergence of the estimated value of the lumped uncertainty to it real values. The persistent excitation condition [16] should be satisfied for the estimated value to converge to its theoretic value.

In order to train the RNN effectively, an on-line parameter training methodology can be derived using adaptation laws $\dot{\mathbf{O}}$ of above the Lyapunov stability theorem. Then adaptation laws of the parameters in the RNN, $\dot{\mathbf{O}}(w_{jk}^3, w_{ij}^2, w_j^2)$ can be computed by the gradient descent method and the backpropagation algorithm as follows

$$\dot{w}_{jo}^3 = \eta z_2 \mathbf{\Gamma} \underline{\Delta} - \eta \frac{\partial V_3}{\partial U_R} \frac{\partial U_R}{\partial y_k^3} \frac{\partial y_k^3}{\partial net_k^3} \frac{\partial net_k^3}{\partial w_{jk}^3} = -\eta \frac{\partial V_3}{\partial U_R} x_j^3 \quad (36)$$

The above Jacobian term of controlled system can be rewritten as $\partial V_3 / \partial U_R = -z_2$. The error term can be calculation as

$$\delta_k \underline{\Delta} - \frac{\partial V_3}{\partial U_R} \frac{\partial U_R}{\partial y_k^3} = z_2 \quad (37)$$

The recurrent weight of hidden layer w_j^2 can be updated as

$$\dot{w}_j^2 \equiv -\frac{\partial V_3}{\partial w_j^2} = -\frac{\partial V_3}{\partial U_R} \frac{\partial U_R}{\partial y_k^3} \frac{\partial y_k^3}{\partial net_k^3} \frac{\partial net_k^3}{\partial y_j^2} \frac{\partial y_j^2}{\partial w_j^2} = \delta_k w_{jk}^3 P_j \quad (38)$$

where $P_j \equiv \partial y_j^2 / \partial w_j^2$ can be calculate from (25). The weight between hidden layer and input layer can be updated as

$$w_{ji}^2 \equiv -\frac{\partial V_3}{\partial w_{ji}} = -\frac{\partial V_3}{\partial U_R} \frac{\partial U_R}{\partial y_k^3} \frac{\partial y_k^3}{\partial y_j^2} \frac{\partial y_j^2}{\partial w_{ji}^2} = \delta_k w_{jk}^3 Q_{ji} \quad (39)$$

where $Q_{ji} \equiv \partial y_j^2 / \partial w_{ji}^2$ can be calculate from (25).

3.2. Experimental Results

A block diagram of the of a DSP control system for a PMSM drive is depicted in Fig. 1. A host PC downloads the program running on the DSP. The proposed controllers are implemented by DSP control system. The current-controlled PWM VSI is implemented by the IGBT power modules with a switching frequency of 15kHz. A DSP control board includes multi-channels of D/A and encoder interface circuits. The PMSM used in this drive system is a three-phase two-pole 220V 750W 2.8A 3600rpm type. The parameters of the PMSM are given as $K_t = 0.62 Nm/A$, $R = 0.98\Omega$, $L_d = L_q = 22.25 mH$. For the convenience of controller design, position and speed signals in the control loop are set at 1V=50rad and 1V=50rad/sec, respectively. The results turn out to be $\overline{K}_t = 0.62 Nm/A$, $\overline{J} = 1.02 \times 10^{-3} Nms^2 = 0.051 Nmsrad/V$, $\overline{B} = 4.06 \times 10^{-3} Nms/rad = 0.203 Nm/V$. The parameters of the proposed integral backstepping control system using RNN uncertainty observer are given in the following:

$$c_1 = 2,\ c_2 = 1,\ \rho = 0.2,\ \eta = 0.1 \quad (40)$$

All the gains in the integral backstepping control system and the ARNNUO based integral backstepping control system are chosen to achieve the best transient control performance in experimentation considering the requirement of stability. The node numbers of the adaptive RNNUO have three, thirty and one neurons at the input, hidden and output layers, respectively. Usually, some heuristics can be used to roughly initialize the parameters of the adaptive RNNUO for practical applications in the experimental results. The control objective is to control the rotor to 6.28 *rad* periodically. Then, when the command is a sinusoidal reference trajectory, the reference model is set to be unit gain. The sampling interval of the control processing in the experimentation is set at 1msec. Some experimental results are provided to demonstrate the control performance of the proposed control systems. Two conditions are provided in the experimentation here, one being the nominal condition, another being the increasing of the rotor inertia and viscous friction to approximately 4 times the nominal value. The experimental results of the integral backstepping control system due to periodic step and sinusoidal command at the nominal case and the parameter variation case are shown in Figs. 6 and 7, respectively. The position responses of the rotor at the nominal case and the parameter variation case are shown in Figs. 6(a), 6(c); 7(a) and 7(c), the associated control efforts are shown in Figs. 6(b), 6(d), 7(b) and 7(d). Though favorable tracking responses can be obtained by the integral

backstepping control system, the chattering in the control efforts are serious due to large control gain. Moreover, the chattering control efforts will wear the bearing mechanism and might excite unstable system dynamics. The experimental results of the ARNNUO based integral backstepping control system due to periodic step and sinusoidal command at the nominal case and the parameter variation case are shown in Figs. 8 and 9, respectively.

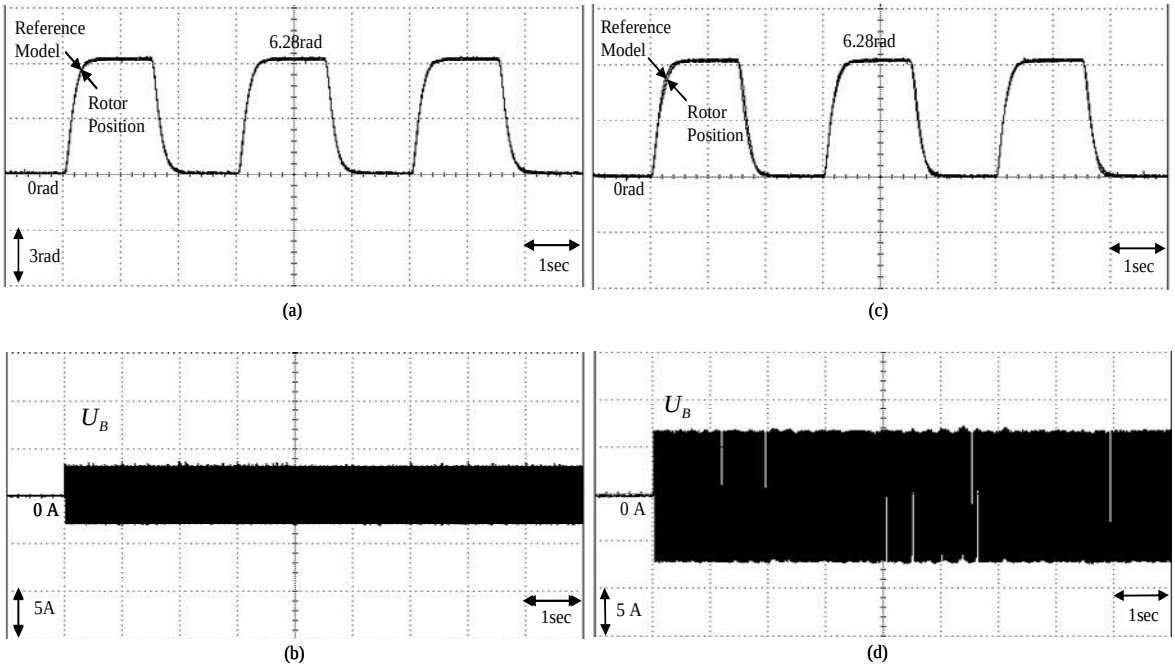

Figure 6. Experimental results of the integral backstepping control system due to periodic step command: (a) rotor position at nominal case; (b) control effort at nominal case; (c) rotor position at parameter variation case; (d) control effort at parameter variation case.

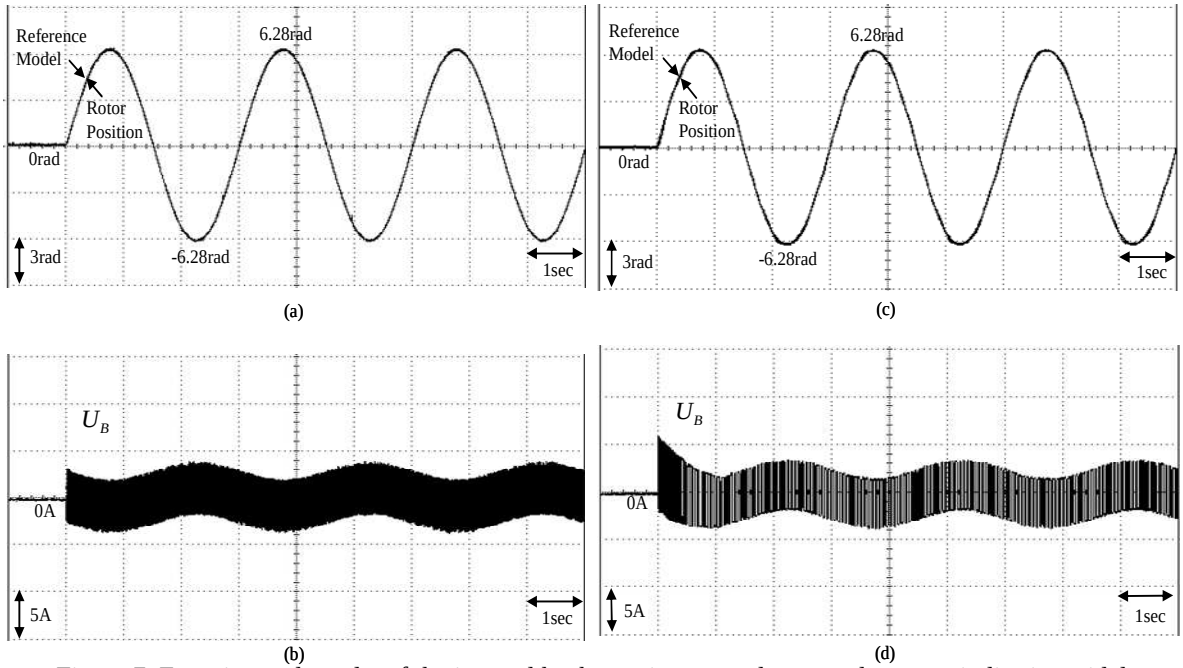

Figure 7. Experimental results of the integral backstepping control system due to periodic sinusoidal command: (a) rotor position at nominal case; (b) control effort at nominal case; (c) rotor position at parameter variation case; (d) control effort at parameter variation case.

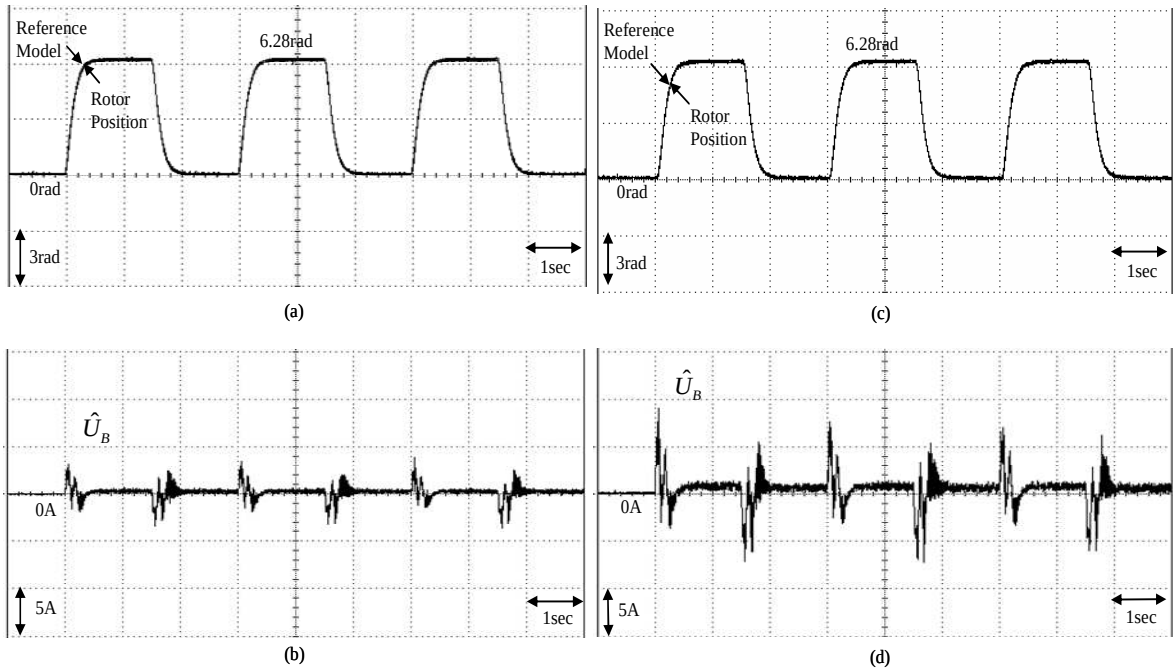

Figure 8. Experimental results of the ARNNUO based integral backstepping control system due to periodic step command: (a) rotor position at nominal case; (b) control effort at nominal case; (c) rotor position at parameter variation case; (d) control effort at parameter variation case.

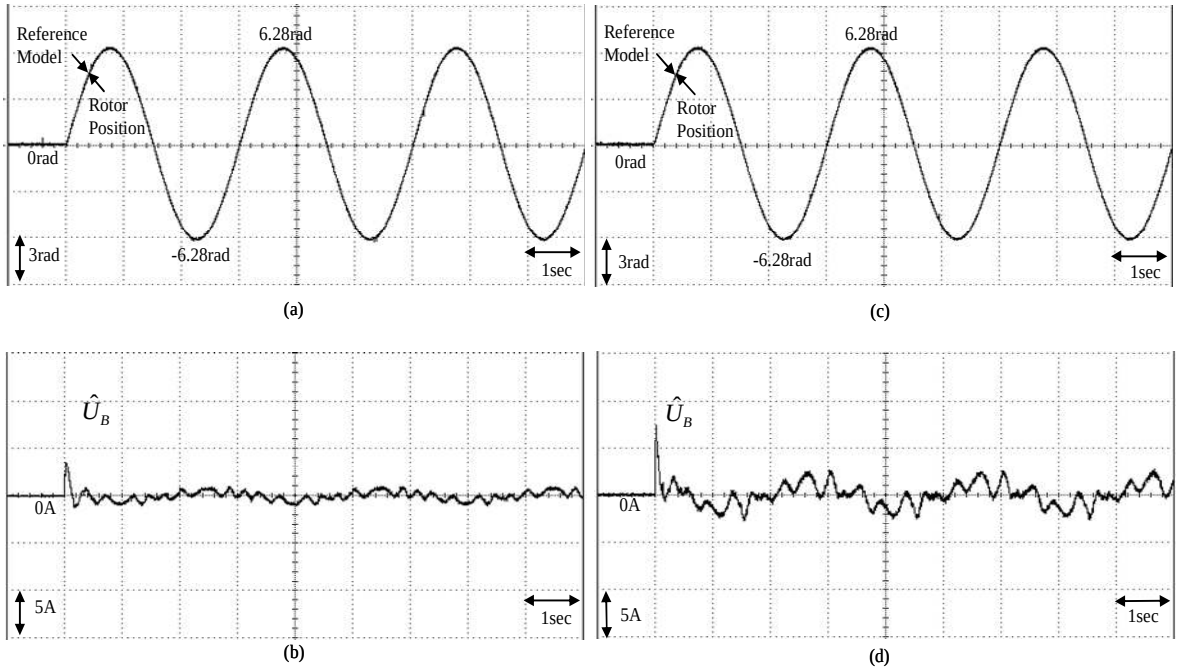

Figure 9. Experimental results of the the ARNNUO based integral backstepping control system due to periodic sinusoidal command: (a) rotor position at nominal case; (b) control effort at nominal case; (c) rotor position at parameter variation case; (d) control effort at parameter variation case.

The position responses of the rotor at the nominal case and the parameter variation case are shown in Figs. 8(a), 8(c); 9(a) and 9(c), the associated control efforts are shown in Figs. 8(b), 8(d), 9(b) and 9(d). Since all the parameters of the RNN are initialized using the pre-trained data, accurate tracking control performance of the PMSM servo drive can be obtained in the first cycle. Moreover, the chattering is much reduced in the

control efforts of the ARNNUO based integral backstepping control system shown in Figs. 8(b), 8(d), 9(b) and 9(d). The transient response of the ARNNUO based integral backstepping control better than the integral backstepping control. However, the robust control performance of the proposed ARNNUO based integral backstepping control system under the occurrence of parameter variations are obvious owing to the on-line adaptive adjustment of the RNN uncertainty observer.

4. CONCLUSIONS

Due to uncertainties existed in the applications of the PMSM drive system which seriously influence the control performance, an ARNNUO based integral backstepping control system is proposed to control PMSM drive system in this paper. First, the field-oriented mechanism is applied to formulate the dynamic equation of the PMSM servo drive. Then, an integral backstepping approach is proposed to control the motion of PMSM drive system. Though favorable tracking responses can be obtained by the integral backstepping control system, the chattering phenomena in the control efforts are serious due to large control gain. Moreover, the chattering control efforts will wear the bearing mechanism and might excite unstable system dynamics. Therefore in order to reduce the chattering in the control efforts and further increase the robustness of the PMSM drive, an ARNNUO is proposed to estimate the required lumped uncertainty. The robust control performances of the proposed RNNUO based integral backstepping control system is obviously under the occurrence of parameter variations for a PMSM drive owing to the on-line adaptive adjustment of the RNNUO. The effectiveness of the proposed control scheme is verified by experimental results.

ACKNOWLEDGEMENTS

The author would like to acknowledge the financial support of the National Science Council in Taiwan, R.O.C. through its grant NSC 99-2221-E-239-040-MY3.

REFERENCES

[1] D. W. Novotny *et al.*, *Vector Control and Dynamics of AC Drives,* New York: Oxford University Press, 1996.
[2] W. Leonhard, *Control of Electrical Drives,* Berlin: Springer-Verlag, 1996.
[3] F. J. Lin, "Real-Time IP Position Controller Design with Torque Feedforward Control for PM Synchronous Motor," *IEEE Transactions on Industrial Electronics,* vol. 44, no. 3, pp. 398-407, June 1997.
[4] M. Krstic *et al.*, "Adaptive Nonlinear Design with Controller-Identifier Separation and Swapping," *IEEE Transactions on Automatic Control,* vol. 40, pp. 426-440, March 1995.
[5] A. Stotsky *et al.*, "The Use of Sliding Modes to Simplify the Backstepping Control Method," in *Proceedings of the 1997 American Control Conference.* 1997, pp. 1703–1708.
[6] G. Bartolini, *et al.*, "Peoperties of a Combined Adaptive/Second-Order Sliding Mode Control Algorithm for Some Classes of Uncertain Nonlinear Systems," *IEEE Transactions on Automatic Control,* vol. 45, pp. 1334–1341, July 2000.
[7] F. J. Lin *et al.*, "Adaptive Backstepping Sliding Mode Control for Linear Induction Motor Drive," *IEE Proceedings Electric Power Appications,* vol. 149, pp. 184–194, May 2002.
[8] C. C. Wang *et al.*, "Chaos Control in AFM System Using Sliding Mode Control by Backstepping Design," *Communications in Nonlinear Science and Numerical Simulation,* vol. 15, pp. 741-751, 2010.
[9] C. L. Chen *et al.*, "High-order Sliding Mode Controller with Backstepping Design for Aeroelastic Systems," *Communications in Nonlinear Science and Numerical Simulation,* vol. 17, pp.1813-1823, 2012.
[10] T. W. S. Chow *et al.*, "A Recurrent Neural-Network-Based Real-Time Learning Control Strategy Applying to Nonlinear Systems with Unknown Dynamics," *IEEE Transactions on Industrial Electronics,* vol. 45, no. 1, pp. 151-161, Feb. 1998.
[11] S. C. Sivakumar *et al.*, "On-Line Stabilization of Block-Diagonal Recurrent Neural Networks," *IEEE Transactions on Neural Network,* vol. 10, no. 1, pp. 167-175, Jan. 1999.
[12] M. A. Brdys *et al.*, "Dynamic Neural Controllers for Induction Motor," *IEEE Transactions on Neural Networks,* vol. 10, no. 2, pp. 340-355, March 1999.
[13] H. Cardot, *Recurrent Neural Networks for Temporal Data Processing*, InTech, Open Access Publisher, 2011.
[14] J. Martens *et al.*, "Learning Recurrent Neural Networks with Hessian-Free Optimization," in *Proceedings of the28th International Conference on Machine Learning,* Bellevue, Washington, USA, 2011.
[15] Q. Liu *et al.*, "Finite-Time Convergent Recurrent Neural Network with a Hard-Limiting Activation Function for Constrained Optimization with Piecewise-Linear Objective Functions," *IEEE Transactions on Neural Network,* vol. 22, no. , pp. 601-613, April 2011.
[16] K. J. Astrom *et al.*, *Adaptive Control,* New York: Addison-Wesley, 1995.

BIOGRAPHY OF AUTHORS

Chih-Hong Lin received the B.S. and M.S. degree in electrical engineering from the National Taiwan University of Science and Technology, Taipei, Taiwan, R.O.C., and the Ph.D. degree in electrical engineering from the Chung Yuan Christian University, Chung Li, Taiwan, R.O.C., in 1989, 1991 and 2001, respectively. He is currently an associate Professor in the electrical engineering, National United University, Miao Li, Taiwan, R.O.C. His research interests include power electonics, motor servo drives and intelligent control.

Ren-Cheng Wu received the B.S. degree in electrical engineering from the National United University, Miaoli, Taiwan, R.O.C., in 2011, He is currently working toward the M.S. degree in the National University University, Miaoli, Taiwan, R.O.C. His current research interests include power electonics, motor servo drive system, and motor control.